

Structure of the sigma meson from lattice QCD

SCALAR Collaboration : Teiji Kunihiro^a, Shin Muroya^b, Atsushi Nakamura^c, Chiho Nonaka^{d,e}, Motoo Sekiguchi^f, Hiroaki Wada^g and Masayuki Wakayama^{*d}

^a*YITP, Kyoto University, Kyoto 606-8502, Japan*

^b*Matsumoto University, Matsumoto 390-1295, Japan*

^c*IMC, Hiroshima University, Higashi-Hiroshima 739-8521, Japan*

^d*Department of Physics, Nagoya University, Nagoya 464-8602, Japan*

^e*Kobayashi Maskawa Institute, Nagoya University, Nagoya 464-8602, Japan*

^f*School of Science and Engineering, Kokushikan University, Tokyo 154-8515, Japan*

^g*Faculty of Political Science and Economics, Kokushikan University, Tokyo 154-8515, Japan*

Our purpose is to obtain insights of structure of the sigma meson from the first principle calculation, lattice QCD. At present we do not reach a conclusive understanding of nature of the sigma meson. Currently it is considered as a usual two-quark state, four-quark states such as a tetra-quark and mesonic molecules or superposition of them. Besides, the mixing with glueballs is one of important and interesting ingredients for structure of the sigma meson. Furthermore, a disconnected diagram of the sigma meson plays an important role in the structure of the sigma meson. However, to evaluate the disconnected part of the propagator is not an easy task in lattice QCD calculation. To compute the disconnected part of the propagator, we use the Z_2 noise method and the time dilution for estimating the all-to-all quark propagators. Here, we focus on four-quark states in the sigma meson. From investigation of two-quark and four-quark states with the inclusion of disconnected diagrams, we will discuss the structure of the sigma meson and the mass of it.

31st International Symposium on Lattice Field Theory - LATTICE 2013

July 29 - August 3, 2013

Mainz, Germany

*Speaker. E-mail: wakayama@hken.phys.nagoya-u.ac.jp (M. Wakayama)

1. Introduction

Since many light scalar mesons such as $\sigma(600)$, $\kappa(800)$, $f_0(980)$ and $a_0(980)$ were found in experiments [1], a lot of theoretical studies have been devoted to investigation of their states. For the structure of light scalar mesons, in addition to the conventional two quark state from the quark model, several possibilities are proposed [2]; four-quark states, molecular states and scattering states. Because the sigma meson is considered as a chiral partner of the pion in the mechanism of hadron mass generation, it is interesting to investigate a roll of four-quark states in the mechanism. The study of four-quark states in light scalar mesons gives us a chance to get an insight of important QCD feature.

After Alford and Jaffe suggested the possibility that scalar mesons exist as four-quark states from the quenched lattice QCD [3], tetra-quark search on the lattice started actively. However, in Ref. [4] they found that the scalar meson exists as no bound states from the dependence of bound energies for four-quark states on the ratio of pion mass and rho meson mass (m_π/m_ρ) and pion mass (m_π). The pioneer work of the sigma meson in full QCD was done by SCALAR collaboration [5]. They showed that disconnected diagrams which contain effectively four-quark states, glueballs and so on make the sigma meson lighter. To understand the sigma meson structure, the full QCD calculation and the evaluation of the disconnected diagram are indispensable. Investigations for the light scalar mesons on full QCD were done in Refs. [5, 6, 7, 8, 9, 10]. Recently using tetra-quark interpolators, not only ground states but also resonance states of scalar mesons on the lattice were reported [8]. However there is no study including all possible structure of the sigma meson at the same time. Here we will show the first full QCD lattice calculation including two-quark, tetra-quark and molecular states in the sigma meson.

2. Propagators of the sigma meson

First we show the formulation of propagators of sigma meson in terms of two quarks. The two-quark propagators of the sigma meson are given by

$$G_{S_1 S_2}^{\text{two-two}}(t) = \left\langle \mathcal{O}_{S_2}^{\text{two}}(t) \mathcal{O}_{S_1}^{\text{two}\dagger}(0) \right\rangle, \quad (2.1)$$

where $\mathcal{O}_S^{\text{two}}(t)$ are two-quark operators and the index S indicates the choice of parameters in the smearing method. The two-quark operators are given by

$$\mathcal{O}_S^{\text{two}}(t) = \frac{1}{\sqrt{2}} \sum_{\mathbf{x}, \mathbf{y}, a, b, \alpha} \left[\bar{u}_\alpha^a(t, \mathbf{x}) S_t^{ab}(\mathbf{x}, \mathbf{y}) u_\alpha^b(t, \mathbf{y}) + \bar{d}_\alpha^a(t, \mathbf{x}) S_t^{ab}(\mathbf{x}, \mathbf{y}) d_\alpha^b(t, \mathbf{y}) \right], \quad (2.2)$$

where S_t is a Gaussian smearing function [11] at a timeslice t . In this paper, we use the point $(N_p, \kappa_p) = (0, 0)$, narrow $(N_n, \kappa_n) = (15, 0.190)$ and wide $(N_w, \kappa_w) = (20, 0.210)$ sources as smearing parameters [11]. Because the sigma meson channel is described as the superposition of operators with the same quantum numbers, using the variational method, we can extract the detailed information of the structure of the sigma meson. The lowest mode of the sigma meson is written by

$$|\text{lowest mode}\rangle = c_0 |\text{two-quark}\rangle_{\text{point}} + c_1 |\text{two-quark}\rangle_{\text{narrow}} + c_2 |\text{two-quark}\rangle_{\text{wide}}, \quad (2.3)$$

where c_0 , c_1 and c_2 are normalized weights of each operator.

The two-quark propagators of sigma meson are composed of connected parts and disconnected ones

$$G_{S_1 S_2}^{\text{two-two}}(t) = -G_{S_1 S_2}^{\text{conn}}(t) + 2G_{S_1 S_2}^{\text{disc}}(t), \quad (2.4)$$

To calculate the connected diagrams we use the conjugate gradient method, however we can not apply it to the calculation of the disconnected diagrams naively. To obtain the disconnected part efficiently, we use the Z_2 noise method in which we estimate the quark propagators stochastically with some noise vectors.

The sigma meson channel may have also overlap with four-quark states. As four-quark states, we calculate molecular and tetra-quark propagators. Molecular operators consist of two color singlet two-quark operators, whereas tetra-quark operators consist of a color anti-triplet diquark operator and a color triplet anti-diquark operator. The molecular propagators of the sigma meson are defined by

$$G_{S_1 S_2}^{\text{molec-molec}}(t) = \left\langle \mathcal{O}_{S_2}^{\text{molec}}(t) \mathcal{O}_{S_1}^{\text{molec}\dagger}(0) \right\rangle, \quad (2.5)$$

where $\mathcal{O}_S^{\text{molec}}(t)$ are the molecular operators. The molecular operators are given by

$$\mathcal{O}_S^{\text{molec}}(t) = \frac{1}{\sqrt{3}} \left[\mathcal{O}_S^{\pi^+}(t) \mathcal{O}_S^{\pi^-}(t) - \mathcal{O}_S^{\pi^0}(t) \mathcal{O}_S^{\pi^0}(t) + \mathcal{O}_S^{\pi^-}(t) \mathcal{O}_S^{\pi^+}(t) \right], \quad (2.6)$$

where $\mathcal{O}_S^\pi(t)$ are two-quark pion operators written as

$$\begin{aligned} \mathcal{O}_S^{\pi^+}(t) &= - \sum_{\mathbf{x}, \mathbf{y}, a, b} \bar{d}^a(t, \mathbf{x}) \gamma_5 S_t^{ab}(\mathbf{x}, \mathbf{y}) u^b(t, \mathbf{y}), \\ \mathcal{O}_S^{\pi^-}(t) &= \sum_{\mathbf{x}, \mathbf{y}, a, b} \bar{u}^a(t, \mathbf{x}) \gamma_5 S_t^{ab}(\mathbf{x}, \mathbf{y}) d^b(t, \mathbf{y}), \\ \mathcal{O}_S^{\pi^0}(t) &= \frac{1}{\sqrt{2}} \sum_{\mathbf{x}, \mathbf{y}, a, b} \left[\bar{u}^a(t, \mathbf{x}) \gamma_5 S_t^{ab}(\mathbf{x}, \mathbf{y}) u^b(t, \mathbf{y}) - \bar{d}^a(t, \mathbf{x}) \gamma_5 S_t^{ab}(\mathbf{x}, \mathbf{y}) d^b(t, \mathbf{y}) \right]. \end{aligned} \quad (2.7)$$

We define the tetra-quark propagators of the sigma meson as

$$G_{S_1 S_2}^{\text{tetra-tetra}}(t) = \left\langle \mathcal{O}_{S_2}^{\text{tetra}}(t) \mathcal{O}_{S_1}^{\text{tetra}\dagger}(0) \right\rangle, \quad (2.8)$$

where $\mathcal{O}_S^{\text{tetra}}(t)$ are the tetra-quark operators. The tetra-quark operators are given by

$$\mathcal{O}_S^{\text{tetra}}(t) = \sum_a [ud]_S^a(t) [\bar{u}\bar{d}]_S^a(t), \quad (2.9)$$

where $[ud]_S^a(t)$ and $[\bar{u}\bar{d}]_S^a(t)$ are the diquark and anti-diquark operators written as

$$\begin{aligned} [ud]_S^a(t) &= \frac{1}{2} \sum_{\mathbf{x}, \mathbf{y}, b, c, d} \varepsilon^{abc} \left[u^{Tb}(t, \mathbf{x}) C \gamma_5 S_t^{cd}(\mathbf{x}, \mathbf{y}) d^d(t, \mathbf{y}) - d^{Tb}(t, \mathbf{x}) C \gamma_5 S_t^{cd}(\mathbf{x}, \mathbf{y}) u^d(t, \mathbf{y}) \right], \\ [\bar{u}\bar{d}]_S^a(t) &= \frac{1}{2} \sum_{\mathbf{x}, \mathbf{y}, b, c, d} \varepsilon^{abc} \left[\bar{u}^b(t, \mathbf{x}) C \gamma_5 S_t^{cd}(\mathbf{x}, \mathbf{y}) \bar{d}^{Td}(t, \mathbf{y}) - \bar{d}^b(t, \mathbf{x}) C \gamma_5 S_t^{cd}(\mathbf{x}, \mathbf{y}) \bar{u}^{Td}(t, \mathbf{y}) \right], \end{aligned} \quad (2.10)$$

where C is the charge conjugate matrix. These operators have a color index. The tetra-quark operator is defined with the diquark and anti-diquark operators by constructing the color index.

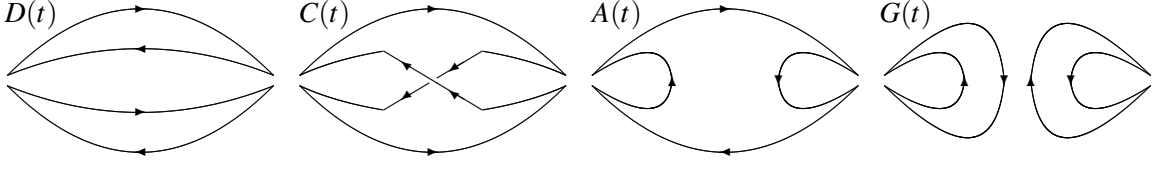


Figure 1: The diagrams for the propagator from the molecular state to the molecular state $G^{\text{molec-molec}}(t)$.

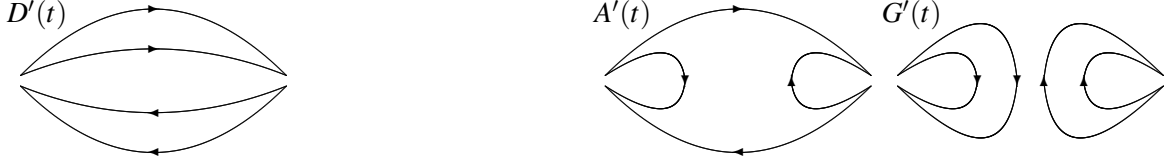


Figure 2: The diagrams for the propagator from the tetra-quark state to the tetra-quark state $G^{\text{tetra-tetra}}(t)$.

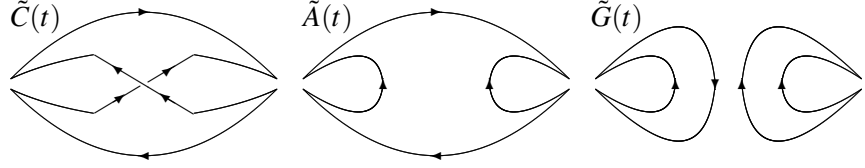


Figure 3: The diagrams for the propagator from the molecular state to the tetra-quark state $G^{\text{molec-tetra}}(t)$.

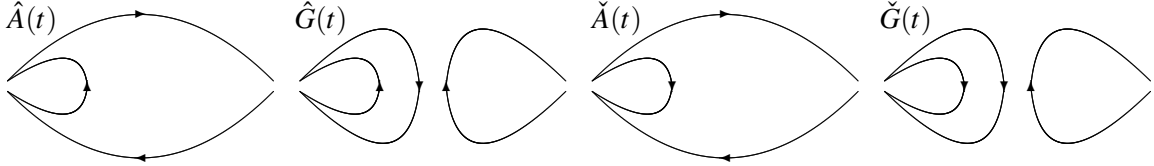


Figure 4: The \hat{A} and \hat{G} diagrams are the propagator from the molecular state to the two-quark state $G^{\text{molec-two}}(t)$. The \check{A} and \check{G} diagrams are the propagator from the tetra-quark state to the two-quark state $G^{\text{tetra-two}}(t)$.

The molecular and tetra-quark propagators are composed of some diagrams,

$$G_{S_1 S_2}^{\text{molec-molec}}(t) = 2 \left[D_{S_1 S_2}(t) + \frac{1}{2} C_{S_1 S_2}(t) - 3A_{S_1 S_2}(t) + \frac{3}{2} G_{S_1 S_2}(t) \right], \quad (2.11)$$

$$G_{S_1 S_2}^{\text{tetra-tetra}}(t) = 2 \left[2(D'_{1S_1 S_2}(t) + D'_{2S_1 S_2}(t)) - 2(A'_{1S_1 S_2}(t) + A'_{2S_1 S_2}(t) + A'_{3S_1 S_2}(t) + A'_{4S_1 S_2}(t)) \right. \\ \left. + (G'_{1S_1 S_2}(t) + G'_{2S_1 S_2}(t) + G'_{3S_1 S_2}(t) + G'_{4S_1 S_2}(t)) \right], \quad (2.12)$$

where D , C , A and G (D' , A' and G') diagrams are shown in Fig. 1 (Fig. 2). The difference between D and D' stands for the difference of the combination of color. We also calculate the diagrams in Figs. 3 and 4, but we do not show the results here. We calculate the disconnected diagrams with the Z_2 noise method. We neglect the doubly disconnected diagrams G or G' which are suppressed by $1/N_c$ compared to singly disconnected diagrams [12].

3. Results

The sigma propagators are calculated on the $N_f = 2$ full QCD gauge configurations which are generated with the Wilson gauge action and the clover quark action. The lattice size is $4^3 \times 8$. The lattice coupling β , the clover coefficient c_{SW} and the hopping parameter κ are set to be $\beta = 1.8$, $c_{SW} = 1.6$ and $\kappa = 0.1409$, respectively. In the calculation of disconnected diagrams, we perform the Z_2 noise method with 960 noise vectors per a quark propagator and the time dilution [13] in the Z_2 noise method. The number of gauge configurations is 8080.

First we investigate the structure of the sigma meson in terms of two-quark state. In left panel of Fig. 5, the disconnected and connected parts of two-quark propagator are shown. We find that the mass of the sigma meson is determined mainly by the disconnected part which makes the mass of the sigma meson lighter. This result is consistent with our previous result which was also computed with point source and point sink [5]. Next we explore the smearing method dependence of the sigma meson structure. We show the two-quark propagators which are composed of disconnected and connected parts with narrow source and sink and wide source and sink together with that with point source and sink in right panel of Fig. 5. We observe that each propagator has the almost the same slope, which suggests the difficulty of obtaining the most dominant state for the lowest mode of the sigma meson just from the propagators. To understand the sigma meson structure in detailed we perform the variational method (Fig. 6) using the propagators. In all temporal region, the weight of point source and sink is smaller, compare to those of narrow and wide sources and sinks. In particular, around $t/a \sim 4, 5$, the signal of the wide source and sink becomes strong. This is a clear evidence that the sigma meson has a spread structure, though it is obtained on the small lattice. This result strongly suggests the possibility of four-quark state for the sigma meson.

Finally, in Fig. 7, we show the sigma meson propagators for two-quark, molecular and tetra-quark states which are calculated with point source and sink. Contrary to our observation from two-quark state, we obtain the following mass relation from the propagators: $m_{\text{two}} < m_{\text{molec}} < m_{\text{tetra}}$. Probably too small lattice for calculation of four-quark states with heavy quark mass leads us the unphysical result. To reach the conclusive result we need to carry out the calculation on larger lattice with lighter quark mass and perform the variational method for the two-quark, tetra-quark and molecular propagators.

4. Summary

We investigated the structure of the sigma meson from point of view of two-quark, tetra-quark and molecular states in full QCD. We calculated not only the connected diagrams but also the disconnected ones which are evaluated with the Z_2 noise method. First, from two-quark propagators with point source and sink, we confirmed that mass of the sigma meson is determined mainly by the disconnected part which makes the sigma meson lighter. Using the variational method for two-quark propagators with point, narrow and wide sources and sinks, we found the clear evidence that the sigma meson has a spread structure. This result supports the possibility of existence of the four-quark state in the sigma meson. However, from comparison among propagators of two-quark, tetra-quark and molecular states, we observed the following mass relation: $m_{\text{two}} < m_{\text{molec}} < m_{\text{tetra}}$. This is the first full QCD lattice calculation for the sigma meson including two-quark and four-

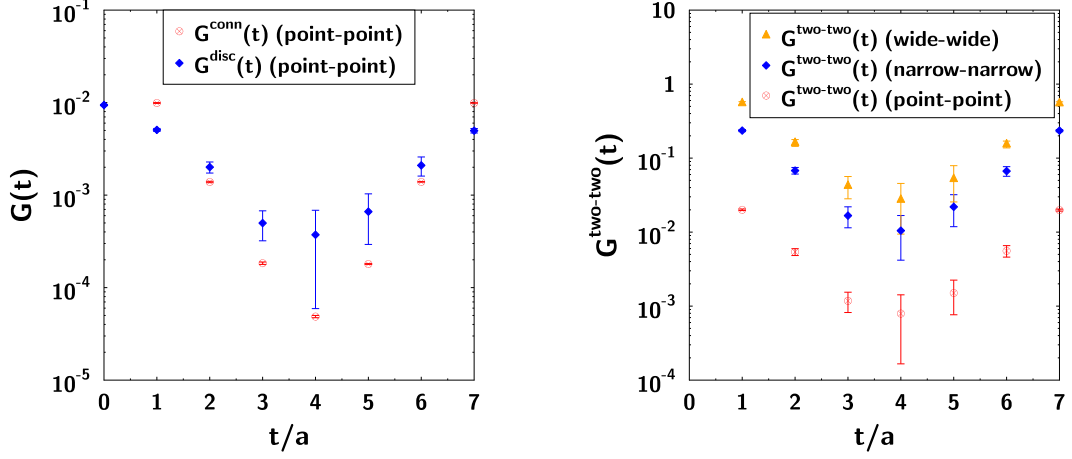


Figure 5: The left figure shows the disconnected (blue solid diamonds) and the connected parts (red open circles) of two-quark propagator with point source and sink. The right figure shows two-quark propagators including of both of connected and disconnected parts which are obtained with point source and sink (red open circles), narrow source and sink (blue solid diamonds) and wide source and sink (orange solid triangles).

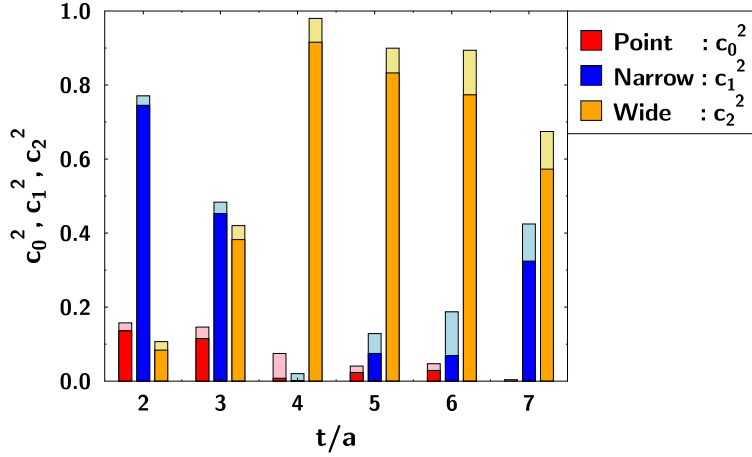


Figure 6: The time dependence of the wights of point source and sink c_0^2 , narrow source and sink c_1^2 and wide source and sink c_2^2 in two-quark propagators.

quark states, though it was done on the small lattice with heavy quark mass. Currently further analyses on a larger lattice with lighter quark mass are on going.

Acknowledgments

This work is supported in part by Nagoya University Program for Leading Graduate Schools "Leadership Development Program for Space Exploration and Research", Grant-in-Aid for Scien-

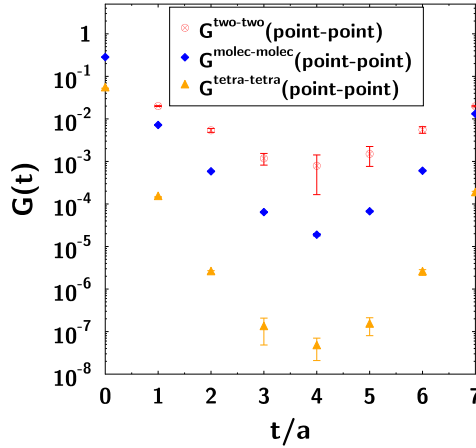


Figure 7: Comparison among two-quark (red open circles), molecular state (blue solid diamonds) and tetra-quark (orange solid triangles) propagators. All of them are calculated with point source and sink.

tific Research (S) (22224003) and the Kurata Memorial Hitachi Science and Technology Foundation. Numerical calculations were performed on the super computers of the Research Center for Nuclear Physics (RCNP), Osaka University.

References

- [1] J. Beringer *et al.* [Particle Data Group Collaboration], Phys. Rev. D **86**, 010001 (2012).
- [2] R. L. Jaffe, Phys. Rev. D **15**, 267 (1977); R. L. Jaffe, Phys. Rev. D **15**, 281 (1977).
- [3] M. G. Alford and R. L. Jaffe, Nucl. Phys. B **578**, 367-382 (2000) [hep-lat/0001023].
- [4] M. Wakayama and C. Nonaka, [hep-lat/1211.2072].
- [5] T. Kunihiro *et al.* [SCALAR Collaboration], Phys. Rev. D **70**, 034504 (2004) [hep-ph/0310312].
- [6] H. Wada *et al.* [SCALAR Collaboration], Phys. Lett. B **652**, 250 (2007).
- [7] A. Hart *et al.* [UKQCD Collaboration], Phys. Rev. D **74**, 114504 (2006).
- [8] G. P. Engel *et al.* [BGR Collaboration], Phys. Rev. D **85**, 034508 (2012).
- [9] S. Prelovsek and D. Mohler, Phys. Rev. D **79**, 014503 (2009).
- [10] C. Alexandrou *et al.* [ETM Collaboration], JHEP **1304**, 137 (2013).
- [11] T. Burch *et al.* [BGR Collaboration], Phys. Rev. D **73**, 094505 (2006).
- [12] Feng-K. Guo, L. Liu, Ulf-G. Meißner and P. Wang, Phys. Rev. D **88**, 074506 (2013).
- [13] J. Foley *et al.* [TrinLat Collaboration], Comp. Phys. Comm. **172**, 145 (2005).